Supplementary Information for

Changes in global DMS production driven by increased CO_2 levels and its impact on radiative forcing

Junri Zhao[1], Yan Zhang[1,2,3*], Shujun Bie[1], Kelsey R. Bilsback[4,5], Jeffrey R. Pierce[4], Ying Chen[1]

[1]*Shanghai Key Laboratory of Atmospheric Particle Pollution and Prevention (LAP3), National Observations and Research Station for Wetland Ecosystems of the Yangtze Estuary, Department of Environmental Science and Engineering, Fudan University, Shanghai 200438, China*

[2]*Shanghai Institute of Eco Chongming (SIEC), Shanghai 200062, China*

[3]*MOE laboratory for National Development and Intelligent Governance, Shanghai institute for energy and carbon neutrality strategy, IRDR ICoE on Risk Interconnectivity and Governance on Weather/Climate Extremes Impact and Public Health, Fudan University, Shanghai 200433, China*

[4]*Department of Atmospheric Science, Colorado State University, Fort Collins, CO, United States of America*

[5]*PSE Healthy Energy, Oakland, CA, United States of America*

Corresponding author: Yan Zhang(yan_zhang@fudan.edu.cn)

Supplementary Methods

Section 1 Description of the projection method

The relationship derived from Figure 1 as follows:

$$\mathrm{Log_{10}DMS} = \begin{cases} -0.727 \times \mathrm{Log_{10}pCO_2} + 2.313, \text{Northern Hemisphere} \\ -2.689 \times \mathrm{Log_{10}pCO_2} + 7.647, \text{Southern Hemisphere} \end{cases} \quad (1)$$

In this study, we established the methodology (Equation S2-S5) for using the pCO_2 and DMS relationship to refine the sea-surface DMS concentrations from CMIP6 ESMs for 2015-2099 under SSP5-8.5 scenario:

$$\mathrm{Log_{10}(PRD)} = \begin{cases} \mathrm{Log_{10}}(\mathrm{DMSO}^{\mathrm{SSP}}_{t-1,i,j}) + K * \mathrm{DeltaX}, K = \begin{cases} -0.727, \mathrm{lat} > 0 \\ -2.689, \mathrm{lat} \le 0 \end{cases} \\ \mathrm{Log_{10}}(\mathrm{DMSO}^{\mathrm{SSP}}_{t,i,j}) \end{cases} \quad (2)$$

$$\mathrm{DeltaX}=\mathrm{Log_{10}}\ (\mathrm{pCO_2}^{\mathrm{SSP}}_{t,i,j})- \mathrm{Log_{10}}\ (\mathrm{pCO_2}^{\mathrm{SSP}}_{t-1,i,j}) \quad (3)$$

$$\mathrm{DeltaY}=\mathrm{Log_{10}}\ (\mathrm{DMSO}^{\mathrm{SSP}}_{t,i,j})- \mathrm{Log_{10}}\ (\mathrm{DMSO}^{\mathrm{SSP}}_{t-1,i,j}) \quad (4)$$

$$\mathrm{Slope}=\mathrm{DeltaY}/\mathrm{DeltaX} \quad (5)$$

Where PRD is the refined sea surface DMS concentrations for 2020-2099, $\mathrm{pCO_2}^{\mathrm{SSP}}_{t,i,j}$ and $\mathrm{DMSO}^{\mathrm{SSP}}_{t,i,j}$ are the CMIP6 models estimated pCO_2 and sea surface DMS concentrations for 2020-2099, lat and *t* represent the latitude of simulation grid and simulation time, *i* and *j* represent row and column of simulation grid, respectively. To account for the contrasting monthly variations of DMS between the Northern and Southern hemispheres, we calculate the PRD using different multiplicative factors K obtained from Equation S1, which represents the gradient of the linear fit for each dataset in the Northern and Southern hemispheres. If the ratio (Slope) of change in Log_{10}(DMS) (DeltaY) to change in $Log_{10}(pCO_2)$ (DeltaX) in a particular grid cell exceeded the regression slope (K) specified in Equation S1 (-0.727 for the Northern hemisphere and -2.689 for the Southern hemisphere), we recomputed DeltaY using K multiplied by DeltaX. The refined model-predicted sea-surface DMS concentration (PRD) was then determined by adding the refined DeltaY to the DMS concentration from the previous simulation time ($\mathrm{Log_{10}}(\mathrm{DMSO}^{\mathrm{SSP}}_{t-1,i,j})$). Otherwise, the DMS estimates obtained from the ESMs were used. DMS flux was calculated using the empirical formula ($F = C_w \times k_w \times (1-\gamma)$) as introduced in Lana et al.[1]. Where, C_w is the seawater DMS concentrations and k_w is the water side gas transfer velocity and γ is the atmospheric gradient fraction. In this study, we selected the Nightingale et al.[2] parameterization for k_w to represent the DMS emissions over the global ocean.

Section 2 Parameterization scheme for ocean acidification used in ESMs

Regarding the four ESMs employed in this study, all considered the impact of ocean acidification on marine chemistry[3]. However, only CNRM-ESM2-1[4] and NorESM2-LM[5] integrated the effect of pH changes on DMS production based on the straightforward parameterization scheme proposed by Six et al.[6] can be expressed as follow :

$$F=1 + (pH_{act} - pH_{pre}) \times \gamma \quad (5)$$

In online ESM simulations, the DMS production rate is adjusted by a constraint factor (F). This factor is influenced by the simulated local pH (pH_{act}) compared to the monthly mean climatological surface pH (pH_{pre}) from pre-industrial control data. The multiplicative factor (γ), representing the gradient from various mesocosm experiments (0.25, 0.58, and 0.87), affects this adjustment. As anthropogenic CO_2 accumulates in the ocean under the SSP5-8.5 scenario, annual mean pH_{act} decreases, causing oceanic pH to decline over time. Consequently, the constraint factor (F) decreases, ultimately leading to a reduction in DMS concentration. It's important to note that while this pH-dependent constraint parameterization is part of NorESM2-LM, it remains inactive in CMIP6 runs[5,7]. Thus, in this study, among the simulated oceanic DMS concentrations, only those from CNRM-ESM2-1 incorporate the response of DMS production to ocean acidity.

Supplementary Table 1. List of CMIP6 ESMs in this analysis of sea-surface DMS concentration.

Name[source]	Grid resolution	Biogeochem model	Description
CNRM-ESM2-1[4]	362 × 294 longitude/latitude; 75 levels	Pisces 2.s	Prognostic scheme (Model simulate key processes involved in DMS production, including zooplankton grazing, phytoplankton exudation, and cell lysis)
NorESM2-LM[8]	360 × 384; 70 levels	HAMOCC	Prognostic scheme (Model simulate DMS release in the water based on temperature and simulated detritus export production)
MIROC-ES2L[9]	360 × 256 longitude/latitude; 63 levels	OECO ver.2.0	Diagnostic scheme (Model use empirical parameterisation to link sea surface DMS concentration with MLD and sea surface chlorophyll concentration)
UKESM-1-0-LL[10]	360 × 330 longitude/latitude; 75 levels	MEDUSA2	Diagnostic scheme (Model use empirical parameterisation to link DMS concentration with a composite variable comprising the logarithm of the product of Chl concentration, light, and a nutrient term dependent on nitrate concentration)

Supplementary Table 2. Description of simulation

Simulation	Description
REF	DMS emissions on with surface ocean DMS concentration for average of four CMIP6 models.
PROJ	DMS emissions on with surface ocean DMS concentration for average of four CMIP6 models refined by the relationship between pCO_2 and DMS.
ND	DMS emissions turned off.

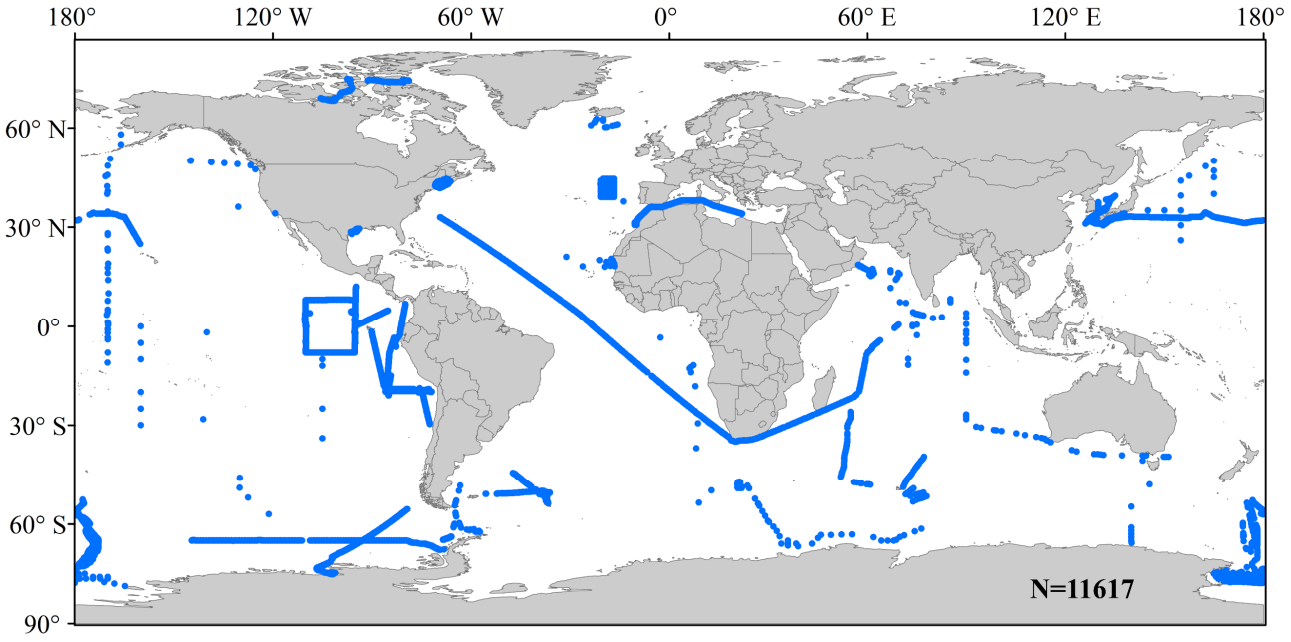

Supplementary Figure 1. Spatial distributions of the match result between pCO_2 and DMS measurements.

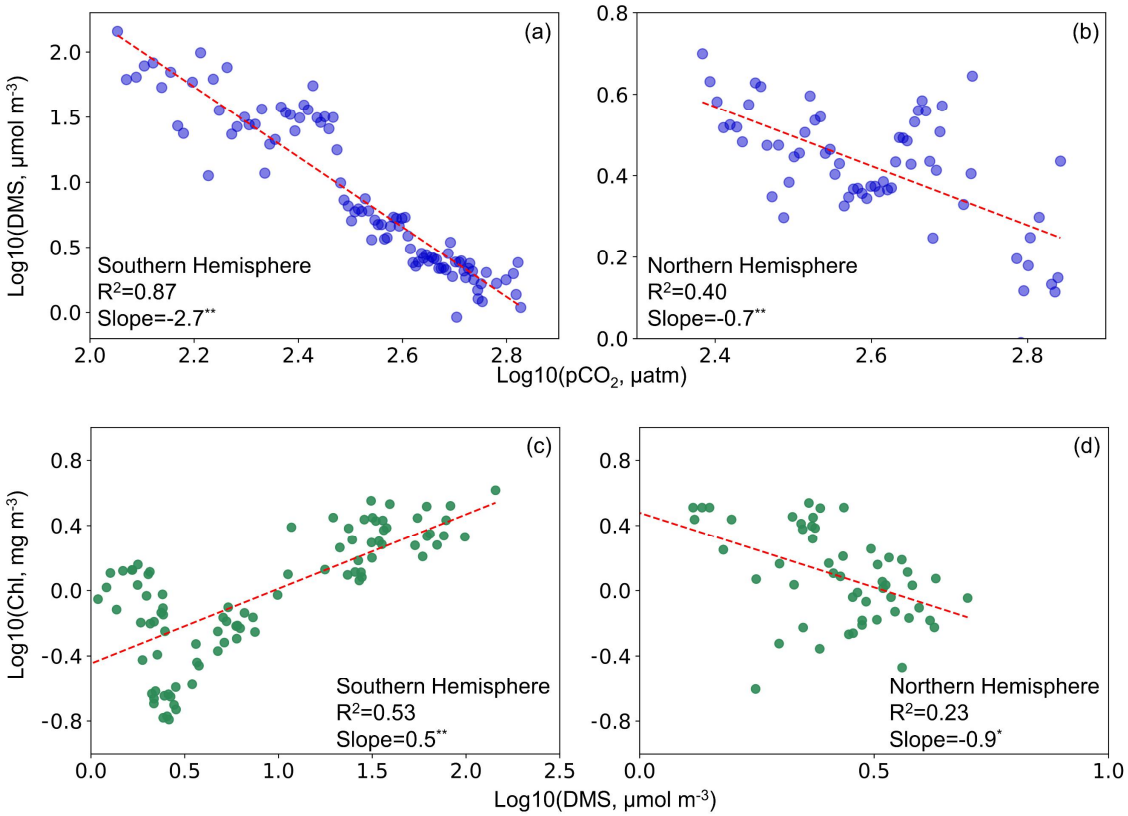

131

132 **Supplementary Figure 2.** Scatter plots depicting the relationships between pCO_2 and DMS (a, b), as well as
133 DMS and Chl (c, d) concentrations in both the Northern and Southern Hemisphere. The red dashed lines indicate
134 the linear regressions between pCO_2 and DMS, as well as DMS and Chl. Significant trends are marked by
135 asterisks (* for $p < 0.05$ and ** for $p < 0.01$). The values of trends are evaluated using the Mann-Kendall test. R^2
136 and Slope represent Pearson's correlation coefficient and the slope of the regression line.

137

138

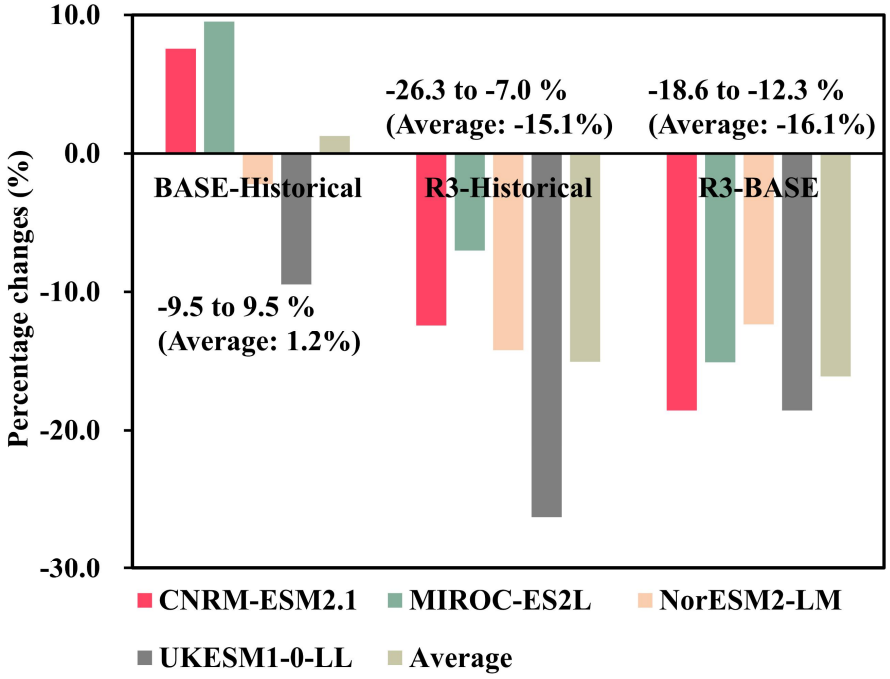

139

140 **Supplementary Figure 3.** Percent changes among Historical, BASE, and PROJ sea-surface DMS concentrations.
141 Historical represent averaged oceanic DMS concentrations from CMIP6 historical experiments of the four
142 models from the year 1960 to 2014. Average represents the mean value of estimated results from four models.

143

144

145

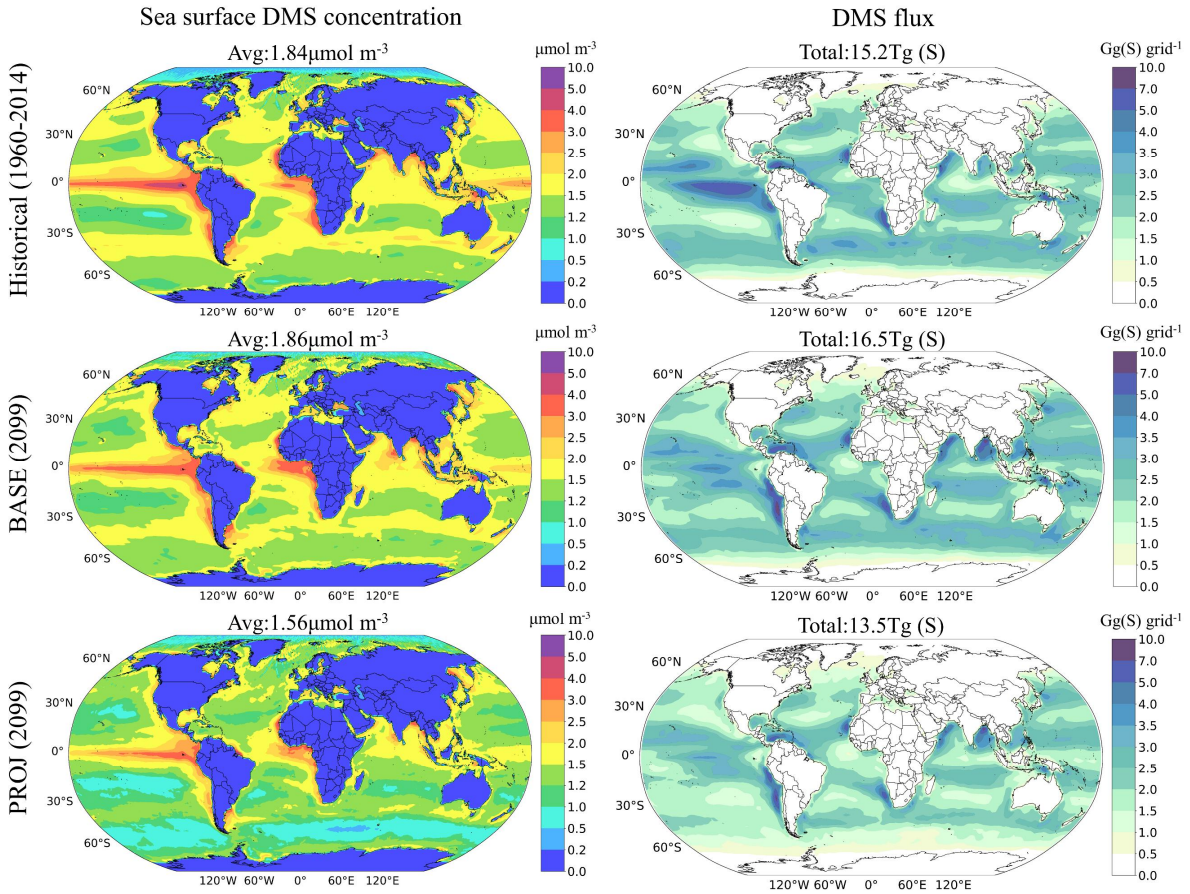

146

147 **Supplementary Figure 4.** The spatial distributions of sea-surface DMS concentrations (first column) and fluxes
148 (second column) from Historical, BASE, and PROJ results.

149

150

151

152

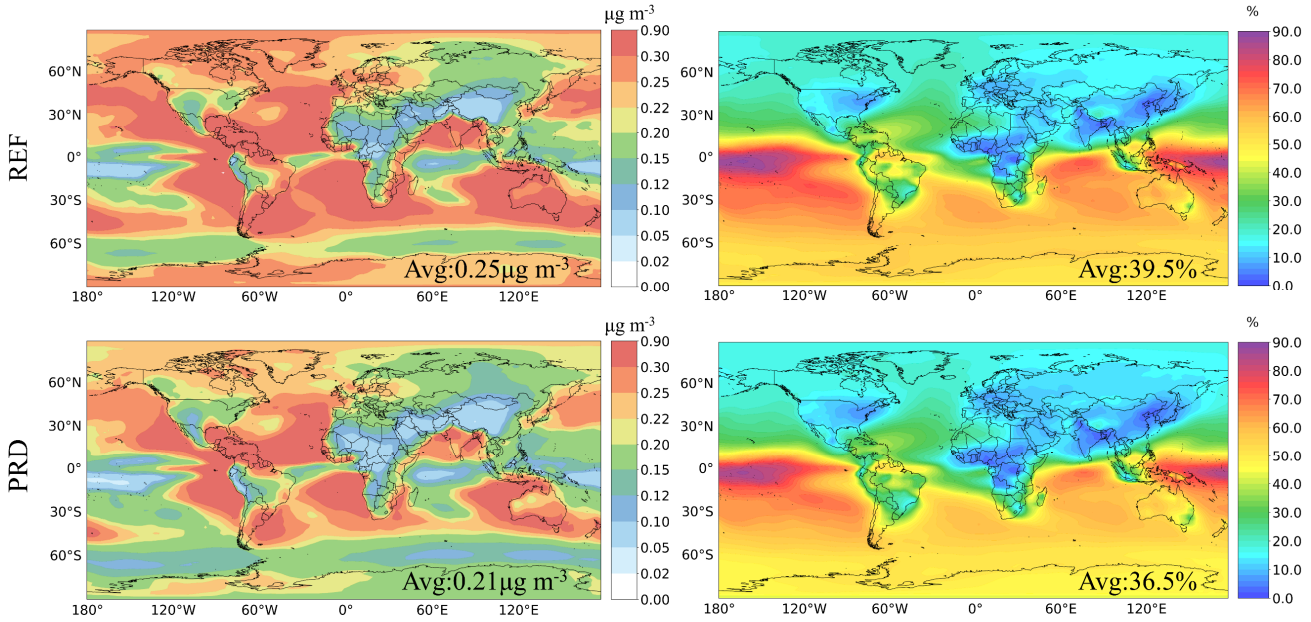

Supplementary Figure 5. The spatial distributions of annual mean absolute in changes surface $SO_4^{2-}$and percent changes N80 (averaged from surface to 100hPa layer) from REF-ND (first row) and PRD-ND (second row) simulation.

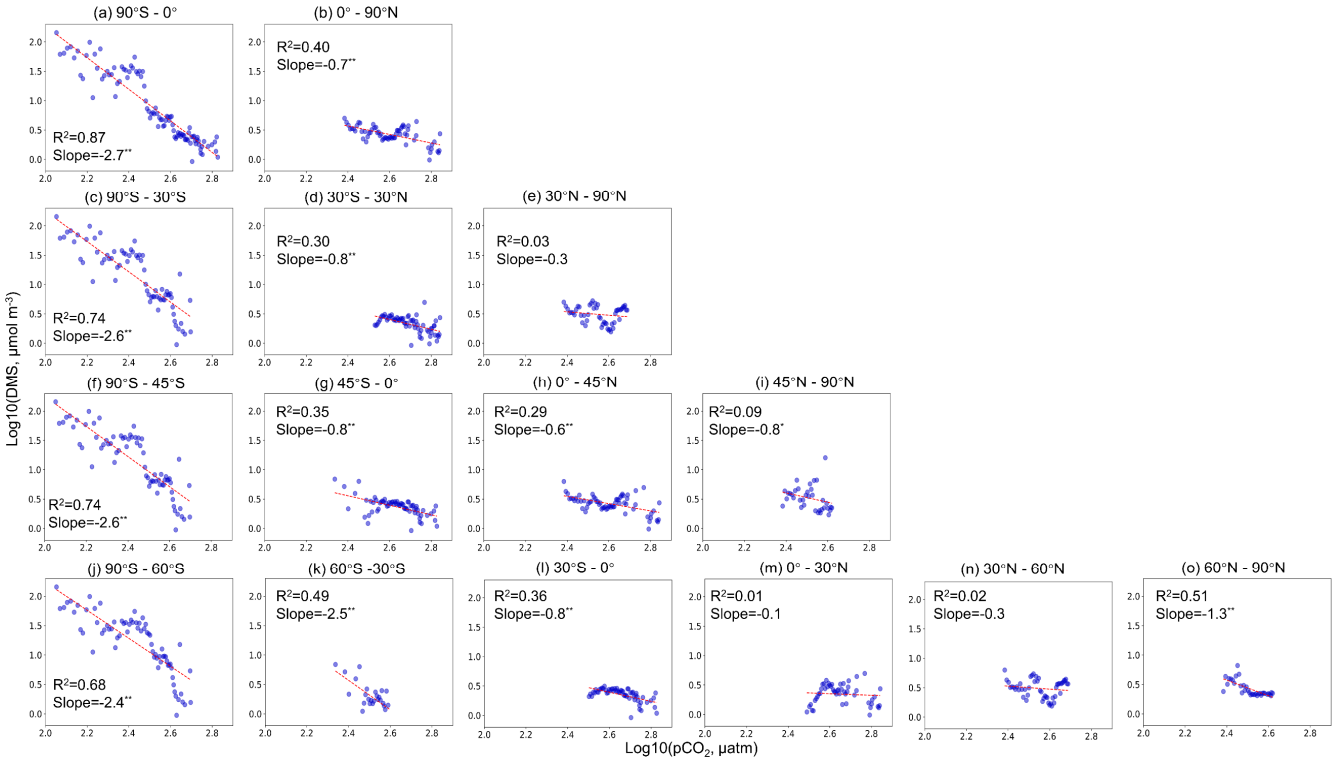

Supplementary Figure 6. The scatter plot of pCO_2 and DMS measurements across various latitudinal zones globally. The red dashed lines indicate the linear regressions between pCO_2 and DMS, as well as pCO_2 and NPP, as estimated by the ESMs. Significant trends are denoted by asterisks (* for $p < 0.05$ and ** for $p < 0.01$), while the absence of an asterisk indicates a lack of significant trend. The values of trends are evaluated using the Mann-Kendall test.

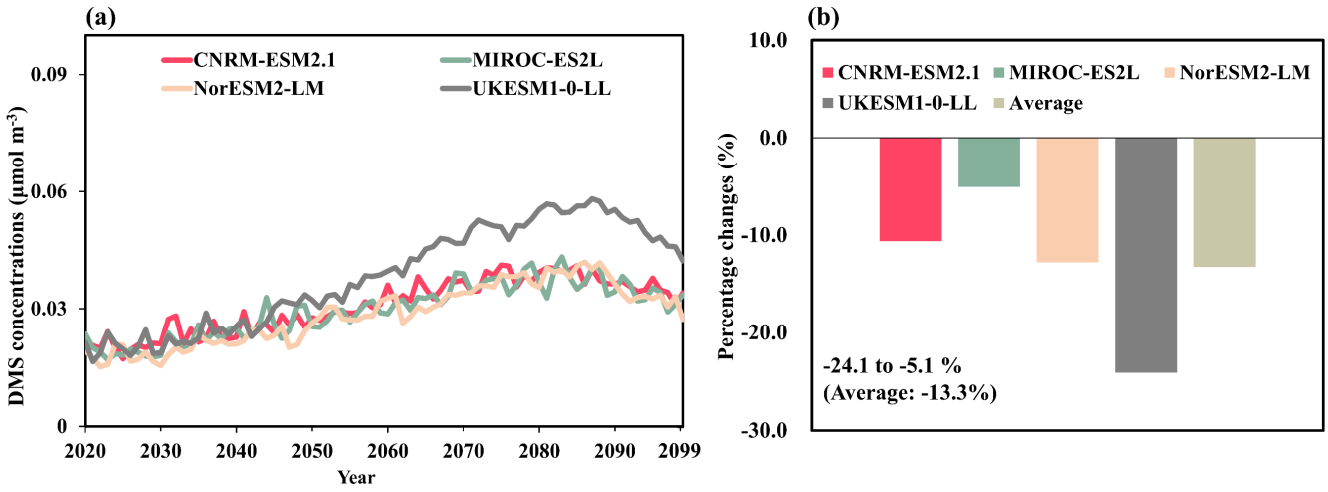

174

175 **Supplementary Figure 7.** Differences between projected sea-surface DMS concentrations using two ratios
176 (Supplementary Figure 2(a,b)) and those using four ratios (Supplementary Figure 6(f-i)) (a). Percent changes
177 between Historical and projected sea-surface DMS concentrations using four ratios (Supplementary Figure 6(f-i))
178 sea-surface DMS concentrations (b). Historical represent averaged oceanic DMS concentrations from CMIP6
179 historical experiments of the four models from the year 1960 to 2014. Average represents the mean value of
180 estimated results from four models.

181

182

183

184

185

186

187

188

189

190

191

192

193

194

Supplementary References

1 Lana, A. *et al.* An updated climatology of surface dimethlysulfide concentrations and emission fluxes in the global ocean. *Global Biogeochem. Cycles* **25,** GB1004 (2011).

2 Nightingale, P. D. *et al.* In situ evaluation of air-sea gas exchange parameterizations using novel conservative and volatile tracers. *Global Biogeochem. Cycles* **14**, 373-387 (2000).

3 Kwiatkowski, L. *et al.* Twenty-first century ocean warming, acidification, deoxygenation, and upper-ocean nutrient and primary production decline from CMIP6 model projections. *Biogeosciences* **17**, 3439-3470 (2020).

4 Séférian, R. *et al.* Evaluation of CNRM Earth System Model, CNRM-ESM2-1: Role of Earth System Processes in Present-Day and Future Climate. *J. Adv. Model. Earth Syst.* **11**, 4182-4227 (2019).

5 Tjiputra, J. F. *et al.* Ocean biogeochemistry in the Norwegian Earth System Model version 2 (NorESM2). *Geosci. Model Dev.* **13**, 2393-2431 (2020).

6 Six, K. D. *et al.* Global warming amplified by reduced sulphur fluxes as a result of ocean acidification. *Nat. Clim. Change* **3**, 975-978 (2013).

7 Bock, J. *et al.* Evaluation of ocean dimethylsulfide concentration and emission in CMIP6 models. *Biogeosciences* **18**, 3823-3860 (2021).

8 Seland, Ø. *et al.* Overview of the Norwegian Earth System Model (NorESM2) and key climate response of CMIP6 DECK, historical, and scenario simulations. *Geosci. Model Dev.* **13**, 6165-6200 (2020).

9 Hajima, T. *et al.* Development of the MIROC-ES2L Earth system model and the evaluation of biogeochemical processes and feedbacks. *Geosci. Model Dev.* **13**, 2197-2244 (2020).

10 Sellar, A. A. *et al.* Implementation of U.K. Earth System Models for CMIP6. *J. Adv. Model. Earth Syst.* **12**, e2019MS001946 (2020).